Unscented Kalman Filter state and parameter estimation in a photobioreactor for microalgae production ⋆

Giancarlo Marafioti [*] **Sihem Tebbani** [**] **Dominique Beauvois** [**]
Giuliana Becerra[**, ***] **Arsene Isambert** [***] **Morten Hovd** [*]

[*] *Department of Engineering Cybernetics, Norwegian University of Science and Technology, N-7491 Trondheim, Norway* {giancarlo.marafioti, morten.hovd}@itk.ntnu.no
[**] *Control Department, SUPELEC, Plateau de Moulon, 91192 Gif sur Yvette, France* {sihem.tebbani, dominique.beauvois, giuliana.becerra}@supelec.fr
[***] *LGPM, Ecole Centrale Paris, 92295 Chatenay-Malabry, France* arsene.isambert@ecp.fr

Abstract: Microalgae have many applications such as the production of high value compounds (source of long-chain polyunsaturated fatty acids, vitamins, and pigments), in energy production (e.g. photobiological hydrogen, biofuel, methane) or in environmental remediation (especially carbon dioxide fixation and greenhouse gas emissions reduction). However, the photobioreactor microalgae process needs complex and costly hardware sensors, especially for biomass measurement. Thus, state and parameter estimation seems to be a critical issue and is studied in this paper in the case of a culture of the microalga Porphyridium purpureum. This paper is an extension of the previous work of Becerra-Celis et al. (2008) where the principal objective is to design a biomass estimator of this microalga production in a photobioreactor based on the total inorganic carbon measurement.
Unscented Kalman filtering is applied to estimation of states and model parameters, producing better performances in comparison with Extented Kalman filtering. Numerical simulations in batch mode, and real-life experiments in continuous mode have been carried out. Corresponding results are given in order to highlight the performance of the proposed estimator.

Keywords: Unscented Kalman Filter, state and parameter estimation, microalgae photobioreactor

1. INTRODUCTION

In chemical and biochemical processes, often chemical reactions have to be monitored and controlled using different sensor measurements. Typically, measurements of reactant and product concentrations, operating temperatures, pressures, and other parameters are needed. In general, a measurement has to be reliable, i.e. it has to be available and accurate. However, there are several reasons why required measurements may not be reliable. Some of such reasons are the impracticability of building an appropriate sensor due to lack of technology, the difficulty to position the sensor, the associated cost. In such cases, an attempt to use estimation techniques may be done.

Dochain (2003) presents an interesting overview of available results on state and parameter estimation in chemical and biochemical processes. A comparison of several traditional state and parameter estimation approaches is given, discussing pros and cons in different cases, and describing how the most common implementation problems are solved (see Dochain (2003) and references therein). In this work particular attention is given to Kalman filtering. Its application to nonlinear systems is tipically implemented by the well known and widely used Extended Kalman Filter (EKF). Even though there are issues due to the inherent linearization procedure in the algorithm, the scientific and industrial communities have obtained successful EKF applications. However, it is the authors' opinion that in systems with strong nonlinearities it could be interesting to exploit the benefits of the Unscented Kalman Filter (UKF). Thus, the UKF is introduced as a valid EKF alternative, and it is shown how to obtain improvement due to its implementation flexibility, extending then its applicability. The first works introducing the Unscented transformation idea and the UKF algorithm are Julier and Uhlmann (1996), and Julier and Uhlmann (1997). In Wan and Van Der Merwe (2000) several UKF algorithms are described, which could be used for state estimation, parameter estimation, and joint state and parameter estimation. This work aims to present UKF advantages in terms of performance and implementation ease, compared to the EKF. The work of Becerra-Celis et al. (2008) is considered as starting point, where it is shown how to implement an

⋆ The authors wish to acknowledge support from the French-Norwegian research cooperation project AURORA

EKF for state estimation in a photobioreactor. Moreover, experimental data is used to validate the results.

Next section explains how to use the UKF for joint state and parameter estimation. Section 3 describes the photobioreactor used for microalgae production, and its model. Section 4 analyzes the application of the UKF to the photobioreactor. In addition, it is shown that when parameter estimation is considered, the UKF produces improved results, particularly when experimental data, collected from continuous cultures, is used. Finally, conclusions and future work are presented.

2. STATE AND PARAMETER ESTIMATION

Consider the following nonlinear system

$$\begin{aligned}\dot{\xi}(t) &= g(\xi(t), u(t), v_\xi(t)) \\ y(t) &= l(\xi(t)) + n(t)\end{aligned} \tag{1}$$

where ξ is the state vector, u is the input vector, y is the measurement vector, v_ξ is the process noise vector, n is the measurement noise vector, of appropriate dimensions, respectively. Simply stated, the state estimation problem consists to reconstruct the state vector knowing the measurement and input vectors, some information on noise distributions, and the nonlinear functions $g(\cdot)$ and $l(\cdot)$. When the parameters used in the model (1) are uncertain the estimation problem may be more difficult to solve. One method to obtain sufficiently good estimates is to make the estimator algorithm robust with respect to the parameter variations. Another method is to try to estimate the uncertain parameters improving the model accuracy. However, joint parameter and state estimation may lead to observability problems. A general framework to introduce the parameter estimation is to extend the state with the uncertain parameters vector and then estimate the augmented state. In cases where the actual parameters are slowly varying, it is common to model the parameters vector η as a random walk driven by a white noise process $v_\eta(t)$. Thus the following differential equation

$$\dot{\eta}(t) = v_\eta(t) \tag{2}$$

is used to augment the system (1). Associating then a relatively small covariance to $v_\eta(t)$, it is possible to consider the slowly varying nature of the parameters. The section below describes the particular UKF used in this work. The algorithm describes the case of joint parameter and state estimate. The equations are still valid if only state estimate is considered. However, the procedure to augment the state vector and covariance matrix, with the parameter vector and its covariance matrix, respectively, must be omitted.

2.1 Unscented Kalman Filter algorithm

Consider the following discretization of the system (1-2)

$$\begin{aligned}\xi_{k+1} &= f(\xi_k, u_k, v_k^\xi, \eta_k) \\ \eta_{k+1} &= \eta_k + v_k^\eta \\ y_k &= h(\xi_k, \eta_k) + n_k\end{aligned} \tag{3}$$

obtained using an appropriate numerical integration routine. To estimate jointly the state and parameters of the system (3), the following augmented vector is defined:

$$\hat{x}_k^a = [\hat{x}_k',\ v_k{}']' \tag{4}$$

where $\hat{x}_k = [\hat{\xi}_k',\ \hat{\eta}_k']'$ has as elements the state and parameter estimates, respectively. The vector $v_k = [v_k^{\xi'}, v_k^{\eta\prime}]'$ contains the process noises in the evolution of ξ and η. Analogously, the augmented covariance matrix is defined as

$$P_k^a = \begin{bmatrix} P_k^x & P_k^{x,v} \\ P_k^{v,x} & P_k^v \end{bmatrix} \tag{5}$$

where P_k^x consists of the state and parameter error covariances, while P_k^v includes the process noise covariance associated to state and parameters. In addition, the off diagonal entries are cross covariance terms represented by the notation $P_k^{\cdot,\cdot}$. Obviously, all elements of $\hat{x}_k^a$ and P_k^a are of appropriate dimensions.

Given the initial conditions

$$\hat{x}_0^a = \begin{bmatrix} \hat{x}_0 \\ 0_v \end{bmatrix}, \qquad P_0^a = \begin{bmatrix} P_0^x & 0 \\ 0 & P_0^v \end{bmatrix}, \tag{6}$$

the dimension L of the augmented system state $\hat{x}^a$, and the following scalar weigths W_i

$$W_0^{(m)} = \lambda/(L+\lambda) \tag{7}$$

$$W_0^{(c)} = \lambda/(L+\lambda) + (1-\alpha^2+\beta) \tag{8}$$

$$\begin{aligned}W_i^{(m)} &= W_i^{(c)} \\ &= 1/[2(L+\lambda)]\end{aligned} \tag{9}$$

for $i = 1, \ldots, 2L$, $\lambda = \alpha^2(L+\kappa) - L$, and where α, β, κ are parameters to be chosen.

For $k = 1, \ldots, \infty$

- Calculate the sigma points defined as

$$\begin{aligned}\left(\mathcal{X}_{k-1}^a\right)_0 &= \hat{x}_{k-1}^a \\ \left(\mathcal{X}_{k-1}^a\right)_j &= \hat{x}_{k-1}^a + \gamma \left(\sqrt{\mathrm{P}_{k-1}^a}\right)_j \\ \left(\mathcal{X}_{k-1}^a\right)_{j+L} &= \hat{x}_{k-1}^a - \gamma \left(\sqrt{\mathrm{P}_{k-1}^a}\right)_j\end{aligned} \tag{10}$$

  where $\left(\sqrt{\mathrm{P}_{k-1}^a}\right)_j$ is the j-th column ($j = 1, \ldots, L$) of the square root of the augmented covariance matrix (5) at the previous time step. The parameter $\gamma = \sqrt{L+\lambda}$ can be interpreted as a scaling factor used to move the position of sigma points around the mean value $\hat{x}_{k-1}^a$. Finally, the sigma points are regrouped in the following matrix of L rows and $2L+1$ columns:

$$\mathcal{X}_{k-1}^a = \begin{bmatrix} \mathcal{X}_{k-1}^x \\ \mathcal{X}_{k-1}^v \end{bmatrix} \tag{11}$$

  where $\mathcal{X}_{k-1}^x$ contains the sigma point rows associated to state and parameters, and $\mathcal{X}_{k-1}^v$ the sigma point rows associated to the state and parameters process noises.

- Propagate the sigma points through the nonlinear dynamics F[·], and compute the predicted state estimate, where the index i is used to select the appropriate sigma point column:

$$\mathcal{X}_{k|k-1} = \mathrm{F}\left[\mathcal{X}^a_{k-1}, u_{k-1}\right] \tag{12}$$

$$\hat{x}^-_k = \sum_{i=0}^{2L} W_i^{(m)} \mathcal{X}_{i,k|k-1} \tag{13}$$

- Compute the predicted covariance:

$$P^-_k = \sum_{i=0}^{2L} W_i^{(c)} \left[\mathcal{X}_{i,k|k-1} - \hat{x}^-_k\right]\left[\mathcal{X}_{i,k|k-1} - \hat{x}^-_k\right]' \tag{14}$$

- Using the predicted mean (13) and covariance (14), recompute a new set of sigma points as defined in (10-11):

$$\mathcal{X}^-_k = \left[\mathcal{X}^{x\prime}_k, \mathcal{X}^{v\prime}_k\right]' \tag{15}$$

- Instantiate the new sigma points through the observation model H[·], and calculate the predicted measurement:

$$\mathcal{Y}_{k|k-1} = \mathrm{H}\left[\mathcal{X}^-_k\right] \tag{16}$$

$$\hat{y}^-_k = \sum_{i=0}^{2L} W_i^{(m)} \mathcal{Y}_{i,k|k-1} \tag{17}$$

- Obtain the innovation covariance and the cross covariance matrices:

$$P_{\tilde{y}_k\tilde{y}_k} = \sum_{i=0}^{2L} W_i^{(c)} \left[\mathcal{Y}_{i,k|k-1} - \hat{y}^-_k\right]\left[\mathcal{Y}_{i,k|k-1} - \hat{y}^-_k\right]' + P^n \tag{18}$$

$$P_{y_k x_k} = \sum_{i=0}^{2L} W_i^{(c)} \left[\mathcal{X}_{i,k|k-1} - \hat{x}^-_k\right]\left[\mathcal{Y}_{i,k|k-1} - \hat{y}^-_k\right]' \tag{19}$$

where P^n is the measurement noise covariance;

- Perform the measurement update using the regular Kalman filter equations:

$$\mathcal{K}_k = P_{y_k x_k} P^{-1}_{\tilde{y}_k\tilde{y}_k} \tag{20}$$

$$\hat{x}_k = \hat{x}^-_k + \mathcal{K}_k\left(y_k - \hat{y}^-_k\right) \tag{21}$$

$$P^x_k = P^-_k - \mathcal{K}_k P_{\tilde{y}_k\tilde{y}_k} \mathcal{K}'_k \tag{22}$$

In (12), F[·] is the modified nonlinear dynamics of (3). The changes are made to consider the discretization and the augmented state, and also to guarantee the proper propagation of each sigma point. Analogously, in (16) H[·] is the modified observation function. Due to the fact that measurement noise is assumed additive with zero mean, it is possible to write (18). Thus, the algorithm computational complexity is reduced because there is no need to associate more sigma points. Regarding filter design parameters, in most cases typical values are $\beta = 2$, and $\kappa = 0$ or $\kappa = 3 - L$, leaving only the parameter α as free parameter. Moreover, considering that $1 \leq \alpha \leq 10^{-4}$ the tuning of the UKF becomes simpler. For a finer tuning and a more accurate description about the meaning of the UKF parameters one can refer to Wan and Van Der Merwe (2000). Finally, in (11) and (15) a square root of a matrix has to be calculated, thus an appropriate algorithm must be used, for instance the Cholesky factorization.

3. PHOTOBIOREACTOR FOR MICROALGAE PRODUCTION

3.1 Strain and growth conditions

The photobioreactor is used to produce the red microalgae *Porphyridium purpureum* SAG 1830-1A obtained from the Sammlung von Algenkulture Pflanzenphysiologister Institut Universität Göttingen, Germany. The strain is growth and maintained on Hemerick medium (Hemerick (1973)). The pH of the Hemerick medium is adjusted to 7.0 before autoclaving it for 20 minutes at 121 °C. Cultures are maintained at 25 °C in 500 ml flask containing 400 ml culture under continuous light intensity of 70 $\mu E m^{-2} s^{-1}$ and aerated with air containing 1% (v/v) CO_2 at 100 rpm on an orbital shaker. During the exponential growth phase, within an interval of two weeks, 200 ml of culture are transferred to a new flask containing fresh medium.

3.2 Culture conditions and measurements

Figure 1 illustrates the photobioreactor diagram where the growth of cultures is performed. The bubble column photobioreactor has a working height of 0.4 m and a diameter of 0.1 m. The total culture volume is 2.5 l, and the cylindrical reactor, made of glass, has an illuminated area of 0.1096 m^2. To agitate the culture an air mixture with 2% (v/v) CO_2 is continuously supplied at a flow rate of 2.5 $V.V.H$ (gas volume per liquid culture volume per hour). 0.22 μm Millipore filters, appropriate valves and flowmeters are used to filter and to control the air flow rate entering the photobioreactor. Four OSRAM white fluorescent tubes (L30W/72) and three OSRAM pink fluorescent tubes (L30W/77) are arranged around the bubble column as an external light source. The incident light intensity on the reactor surface is measured at ten different locations with flat surface quantum sensors (LI-COR LI-190SA). The average light intensity is computed by the weighted average of all measurements. The optimal value of irradiance on surface for the reactor is 120 $\mu E m^{-2} s^{-1}$. A transparent jacket connected to a thermostat unit allows the temperature control, which is regulated at 25 °C. Other sensors are a pH sensor (Radiometer Analytical) and a dissolved oxygen sensor (Ingold type 170). A sampling port is applied to the top of the column, from where samples for off line analysis are collected after 6, 8, and 12 hours. The number of cells is counted using an optical microscope ZEISS Axioplan-2 on Malassez cells. The total inorganic carbon (T.I.C.) in the culture medium is calculated by gas phase chromatography. This method, proposed by Marty et al. (1995), is used to measure low inorganic carbon concentrations down to $(10^{-6} mol\ l^{-1})$ within an accuracy of 10%.

3.3 Mathematical model

In this work the bioprocess model presented in Baquerisse et al. (1999) is used. It consists of two sub models, one describing the growth kinetics, and one representing the gas-liquid mass transfer in the photobioreactor. This

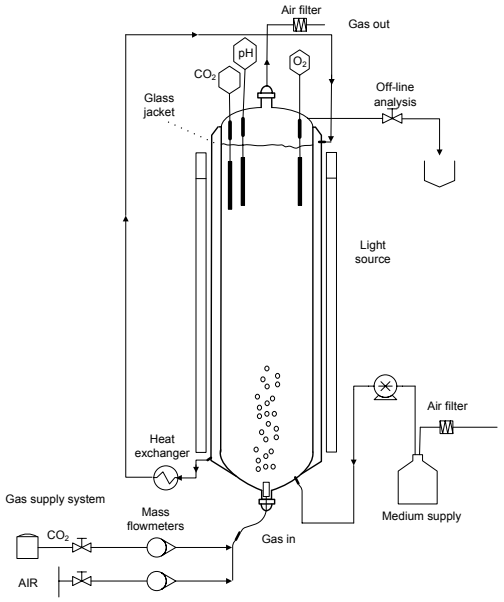

Fig. 1. Photobioreactor diagram.

results in two differential equations describing the state of the reactor:

$$\begin{aligned}\frac{dX}{dt} &= \frac{F_{in}}{V}X_{in} + \mu X - \frac{F_{out}}{V}X \\ \frac{d[TIC]}{dt} &= \frac{F_{in}}{V}[TIC]_{in} - \frac{F_{out}}{V}[TIC]_{out} - \mu\frac{X}{Y_{X/S}} \\ &\quad - mX + k_L a\left([CO_2^*] - [CO_2]\right) \end{aligned} \tag{23}$$

where X is the biomass, and $[TIC]$ is the inorganic carbon concentration associated with cell density increase. The subscripts $[\cdot]_{in}$ and $[\cdot]_{out}$ indicate quantities flowing into, and out from the reactor, respectively. V is the culture volume, and F is the medium flow rate. The mass conversion yield is defined by $Y_{X/S}$, m is the maintenance coefficient, and $k_L a$ is the gas-liquid transfer coefficient. The carbon dioxide concentration in the medium fresh is defined as:

$$[CO_2^*] = \frac{PCO_2}{\mathcal{H}} \tag{24}$$

where PCO_2 is the partial pressure of carbon dioxide, and $\mathcal{H}$ is the Henry's constant for Hemerick medium. Moreover, the carbon dioxide concentration in the medium is given by:

$$[CO_2] = \frac{[TIC]}{\left[1 + \frac{K_1}{[H^+]} + \frac{K_1 K_2}{[H^+]^2}\right]} \tag{25}$$

where K_1, K_2 are kinetics constants, and $[H^+]$ is defined as:

$$[H^+] = 10^{-pH} \tag{26}$$

representing the hydrogen ions concentration in the culture media.

In addition, a light transfer model is considered, which describes the evolution of incident and outgoing light intensity:

$$E = \frac{(I_{in} - I_{out})A_r}{VX} \tag{27}$$

$$I_{out} = C_1 I_{in} X^{C_2} \tag{28}$$

where E is the light "energy" accessible per cell, I_{out} is the outgoing light intensity, I_{in} is the ingoing light intensity. C_1, C_2 are constants depending on the reactor geometry, and A_r is its area.

The light intensity and the total carbon concentration influence the specific growth rate, defined as

$$\mu = \mu_{max}\frac{E}{E_{opt}}e^{\left(1-\frac{E}{E_{opt}}\right)}\frac{[TIC]}{[TIC]_{opt}}e^{\left(1-\frac{[TIC]}{[TIC]_{opt}}\right)} \tag{29}$$

where μ_{max}, E_{opt}, and $[TIC]_{opt}$ are model parameters identified from the batch data experiments. Finally, in (29) substrates limitation effect is taken into account.

3.4 Batch and continuous operating conditions

The photobioreactor can work in two different operating conditions, batch mode and continuous mode. In batch mode:

$$F_{in} = F_{out} = 0; \qquad [TIC]_{in} = 0; \qquad X_{in} = 0. \tag{30}$$

In continuous mode, instead:

$$F_{in} = F_{out} \neq 0. \tag{31}$$

3.5 Model parameters

The model parameters used in this work are the ones identified in Becerra-Celis et al. (2008). For more details on the system identification procedure the reader is referred to their work. Tables 1 and 2 contain the parameters for the microalgae and the total inorganic carbon dynamics, respectively.

Table 1. Model parameters for *Porphyridium purpureum* at 25 °C.

Parameter	Unit	Value
μ_{max}	h^{-1}	0.0337
E_{opt}	$\mu Es^{-1}(10^9 cell)^{-1}$	1.20
$[TIC]_{opt}$	$mmolel^{-1}$	12.93
$k_L a$	h^{-1}	41.40
C_1		0.28
C_2		−0.55

Table 2. Model parameters for [TIC] dynamics.

Parameter	Unit	Value
K_1		$1.02 \cdot 10^{-6}$
K_2		$8.32 \cdot 10^{-10}$
m	$h^{-1}mmole(10^9 cell)^{-1}$	0.004
$Y_{X/S}$	10^9 *cell per mole TIC*	198.1
$\mathcal{H}$	*atm l mole*$^{-1}$	34.03

4. BIOMASS ESTIMATION

Controlling a photobioreactor has some difficulties associated to the implicit nonlinear and time varying nature of the system. There are also problems with the practicability

to find reliable online sensors able to measure the state variables (Shimizu (1996)). To overcome the lack of online sensors, Becerra-Celis et al. (2008) show how to implement an Extended Kalman Filter (EKF) to estimate the biomass for the photobioreactor, described in Section 3, using the measurement of T.I.C.. In this work, it is shown how the use of an UKF gives better performance, particularly for continuous cultures. There are several reasons for which the UKF may be considered as an EKF alternative. There is no linearization procedure in the UKF, as can be seen in section 2.1. This is relevant when strong nonlinearities are present in the process because no linearization error is introduced. It is straightforward to extend the state estimation to joint estimation, just augmenting the estimated vector and covariance matrix, while calculation of system derivatives with respect to the parameters, are required in an EKF algorithm.

4.1 UKF applied to the photobioreactor

Using the UKF, described in Section 2.1, the main objective is to estimate the biomass X in the photobioreactor of Section 3. Focusing on the two different working conditions defined in Section 3.4, it is observed how in batch mode the UKF has an excellent performance, which also is the case for the EKF designed in Becerra-Celis et al. (2008). This is due to the fact that the model parameters are identified in batch mode, and the measurements have a constant sampling time. A more complex scenario appears for continuous cultures. The model parameters are still the ones from the batch experiments, and the experimental data are collected at variable instant intervals. Due to the variable time steps, Becerra-Celis et al. (2008) implements a continuous discrete version of the EKF. In this work, this problem is tackled in two steps. Firstly, a zero order hold is applied to the measurements, secondly the standard UKF algorithm is properly modified. More in detail, the discrete UKF algorithm with an augmented state to consider parameter estimation and process noise is implemented. The sigma points are recomputed in (15) and then used to obtain the predicted measurement in (16-17). Those modifications give the possibility to use the discrete algorithm with the irregular measurement sampling time of the continuous culture case. Furthermore, the parameter μ_{max} in (29) is chosen to be estimated. Finally, despite the fact that a zero order hold is used to permit a discrete UKF implementation, the UKF accuracy and speed of convergence are improved with respect to the EKF ones.

4.2 Simulation results with experimental data

The following results show the efficiency of the proposed method when the photobioreactor works either in batch mode or in continuous mode. Figure 2 illustrates the convergence of the UKF in simulated batch mode, for which conditions (30) hold. In this case the nonlinear model (23) is discretized at sampling time $T_s = 0.5\ h$ and used to simulate the state of the process, starting from initial conditions $X_0 = 2.44 \cdot 10^9 cell/l$, $[TIC]_0 = 2.55\ 10^{-3} mole/l$. After that, $[TIC]$ is corrupted by additive Gaussian white noise with standard deviation $\sigma = 0.2\ 10^{-3} mole/l$, and used as measurement for the UKF. Thus, the state is

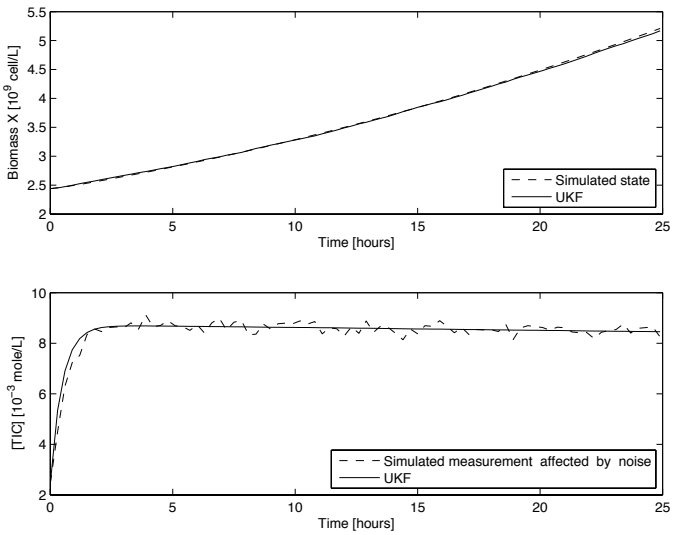

Fig. 2. UKF estimation for simulated batch mode.

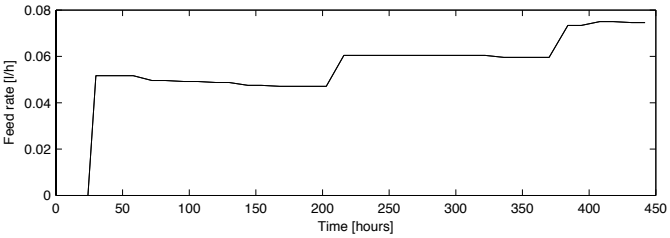

(a) Culture medium feeding profile

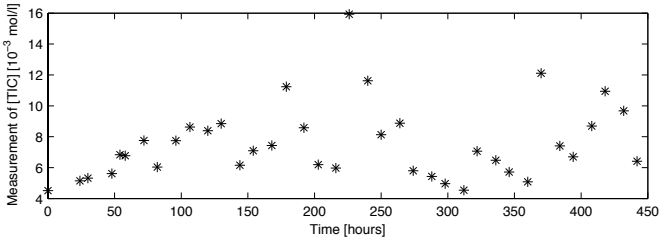

(b) Measurement of [TIC]

Fig. 3. Experimental data: input and output of the photobioreactor collected in continuous mode.

estimated successfully with excellent noise rejection in T.I.C.. The results obtained for continuous cultures are even more interesting. Initial conditions are $X_0 = 1.8 \cdot 10^9 cell/l$, $[TIC]_0 = 4.51 \cdot 10^{-3} mole/l$, and in addition real experiment data, presented in Figure 3, are used as input to the filters. The EKF designed in Becerra-Celis et al. (2008), the UKF with only state estimation, and the UKF with joint state and parameter estimation are simulated. The results obtained are shown in Figure 4 and here discussed. In Figure 4(a) it is noticeable how both UKF implementations have faster speeds of convergence than the EKF. In Figure 4(b) the state estimation error of the three different approaches are compared, and it is evident how the UKFs give smaller estimation errors. Moreover the mean squared error (MSE) between the biomass and its estimate is computed. Table 3 shows the MSE index, which is obtained averaging the MSE along the entire simulation period. From both figures it is noticeable how the UKF performs better than the EKF, and how the introduction

Table 3. Mean Squared Error Index

EKF	UKF	UKF with par. est.
13.60	6.12	6.12

of parameter estimation in the UKF improves the accuracy of the estimation in the final part (after 300 hours), although slightly reduces the speed of convergence. Since the parameters are identified from batch experiments, as shown in Becerra-Celis et al. (2008), adding parameter estimation may be useful when the photobioreactor is run in continuous mode. Figure 5 shows the evolution of the μ_{max} estimation, the estimated value is compared with the identified value and moreover the UKF error covariance is shown.

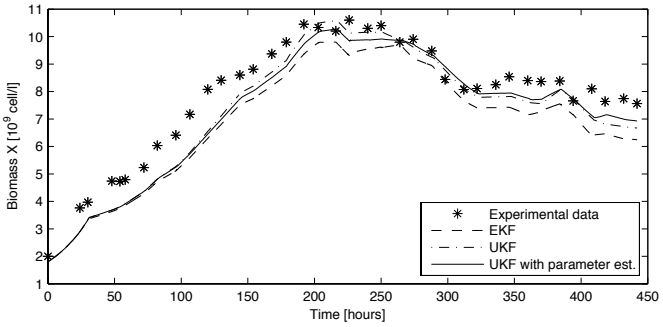

(a) Biomass estimate

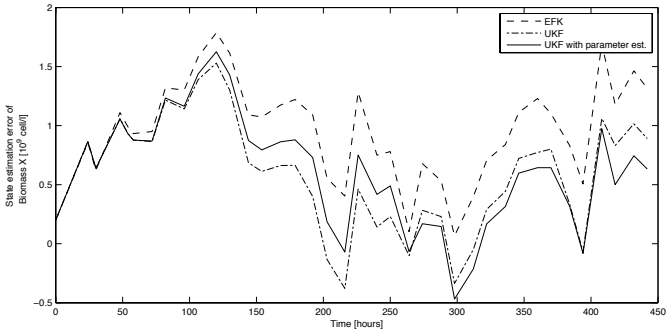

(b) State Estimation Error

Fig. 4. Biomass estimation comparison for continuous cultures.

5. CONCLUSION

This work can be considered as an extension of Becerra-Celis et al. (2008), where the main objective is to design an efficient, reliable and applicable biomass estimator for a microalgae photobioreactor. A more recent nonlinear estimator (UKF) is used, obtaining improved results. In both batch and continuous mode, the approach presented produces a faster estimate convergence and a better estimate accuracy. The capacity and ease to introduce parameter estimation jointly with state estimation, the absence of linearization, the comparable computational complexity make the UKF an attractive estimator for nonlinear systems. The particular UKF framework described in section 2.1 showed to be well suited for the case when measurements, arriving at variable time instants, are subject to a zero holder filter. The extra set of sigma points calculated in (15) are needed to obtain a smoother estimate. Future work is needed to design a feedback based controller using

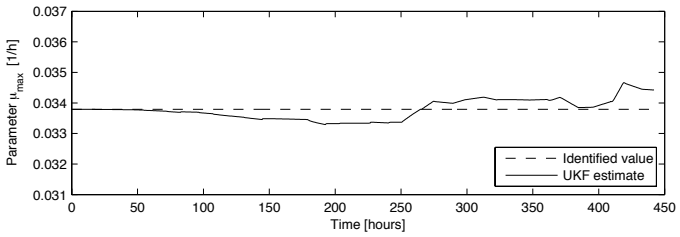

(a) UKF estimate and identified value of μ_{max}

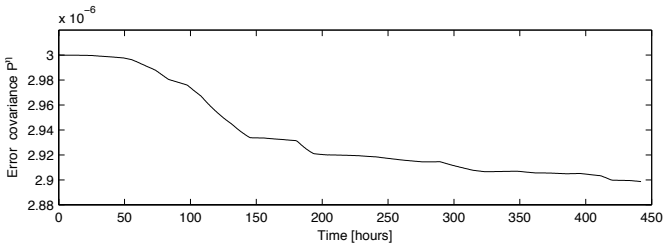

(b) UKF error covariance of μ_{max}

Fig. 5. UKF parameter estimate and its covariance for continuous culture.

the UKF estimate, and to better understand which parameter would improve the filter performance without introducing observability issues. It is also interesting to explore how the UKF performs with other processes compared to the traditional methods in use in practice.

REFERENCES

Baquerisse, D., Nouals, S., Isambert, A., dos Santos, P.F., and Durand, G. (1999). Modelling of a continuous pilot photobioreactor for microalgae production. *Journal of Biotechnology*, 70(1-3), 335 – 342.

Becerra-Celis, G., Tebbani, S., Joannis-Cassan, C., Isambert, A., and Boucher, P. (2008). Estimation of microalgal photobioreactor production based on total inorganic carbon in the medium. *17th IFAC W.C., Seoul*.

Dochain, D. (2003). State and parameter estimation in chemical and biochemical processes: a tutorial. *Journal of process control*, 13, 801 – 818.

Hemerick, J. (1973). Culture methods and growth measurements. In J. Stein (ed.), *Handbook of Physiological Methods*, 250–260. Cambridge University Press, UK.

Julier, S. and Uhlmann, J.K. (1996). A general method for approximating nonlinear transformations of probability distributions. Technical report, .

Julier, S.J. and Uhlmann, J.K. (1997). A new extension of the kalman filter to nonlinear systems. In *Int. Symp. Aerospace/Defense Sensing, Simimulation and Controls*, 182–193.

Marty, A., Cornet, J., Djelveh, G., Larroche, C., and Gros, G. (1995). A gas phase chromatography method for determination of low dissolved CO_2 concentration and/or CO_2 solubility in microbial culture media. *Biotechnology Technique*, 9(11), 787–792.

Shimizu, K. (1996). A tutorial review on bioprocess systems engineering. *Computers and Chemical Engineering*, 20, 915–941.

Wan, E.A. and Van Der Merwe, R. (2000). The unscented kalman filter for nonlinear estimation. *Adaptive Systems for Signal Processing, Communications, and Control Symposium*, 153–158.